CASCADED CONTROL OF COMPLIANT ACTUATORS IN FRIENDLY ROBOTICS

Tao QIAO[1], Shusheng BI[2]

An actuator with compliant element is used for the robot safety when contacting with unknown surroundings, especially for the safety between humans and robots. The compliant element in the compliant actuator can absorb excessive collision force. The robot system should have low stiffness when subjected to a collision force greater than injury tolerance, but otherwise maintain the required capability. For the compliant actuator, system stiffness can be defined as 'mechanical impedance', impedance is the ratio between output force and output shaft angle. The 'impedance' characteristic for collision analysis and stable ability are analyzed in this paper. A cascaded control strategy is adopted for the robustness characteristic. The research shows that, low system stiffness (low mechanical impedance) leads to stable requirement and safety collision outcome. Several methods that can decrease the impedance are provided. Furthermore, saturation is analyzed by adopting saturation operators. The tradeoff of the requirements should considering several indices.

Keywords: compliant actuator, cascaded control, mechanical impedance, collision force, saturation operator

1. Introduction

In traditional applications, actuators are preferred to be as stiff as possible to get high force/torque bandwidth and trajectory tracking control fidelity. However, in many recent applications including robot-human interaction, this kind of actuators is not the optimal choice. Thus, springs are introduced in these systems to get desired characteristic. Such an actuator with mechanical deformation element in the system is called a passive compliance.

Pratt, Robinson and Williamson[1-6]proposed a concept called SEA (Series Elastic Actuator). The SEA with a spring intentionally placed at the actuator output is a low impedance system. Because a compliant element is used in the flexible actuator system, energy can be stored and shocks can be absorbed. In other words, the system with a compliant element leading to a low impedance that force controlled actuation improves safety. These types of actuators are widely used in walking robots[7], prosthetic and orthotic leg systems[8] and force-sensing robot arms[9] and other applications.

[1] Beihang University, China, e-mail: qiaotao21@yahoo.com.cn
[2] Beihang University, China

Compared with a stiff robot system, the manipulator stability of a compliant system is not sufficient for contacting with the unknown environment. The stability analysis of the impedance is necessary. According to Colgate and Hogan's principle, Williamson[2] and Heike Vallery[10] designed controllers to ensure the passivity and the stability. In the applications of walking robots, prosthetic and orthotic leg systems and force-sensing robot arms, these tasks work at low speed and high force density that lead to the use of transmission or gear reduction. Transmissions introduce friction and backlash which are undesirable effects. Backlash between every part of the actuation creates noise and instability. In order to conquer such drawbacks, a cascaded scheme based on torque control main loop and inner velocity control loop is adapted. Gordon Wyeth[11] proposes a new variant of SEA that minimizes the effects of the system backlash, overcoming the stiction effect. Heike Vallery[10] employs a cascaded scheme can ensure passivity and while counteracting static errors, the analysis of the parameters boundaries are emphasized. The cascaded scheme provided by Reza Ghorbani[12] uses saturation operators in the system to ensure minimization of the saturation effects.

As the index of stability and collision, the detailed characteristics of impedance should be further illustrated. Meanwhile, saturation performance reflects whether the analyzed characteristics could be implemented. The characteristics of the system based on cascaded control scheme need a further research. In this paper, to implement these requirements, a cascaded control strategy is described in details in section 2 for analyzing the stability of the whole system and the mechanical impedance in section 3. In section 4, the influence of the parameters for mechanical impedance is expounded elaborately. In order to contacting the collision force and impedance, equations are obtained based on theorem of momentum in section 5. Furthermore, the saturation performance by introducing the saturation operators is well illustrated for analyzing the parameters influence.

2. System model

In this section, cascaded control strategy will be described in details. The series elastic actuator (SEA) joint consists of a DC motor coupled to the load via series elasticity. As shown in Fig.1, the cascaded control strategy has a torque control main loop and a velocity inner loop. The velocity feedback from an encoder forms a velocity loop for controlling the motor and gearbox nonlinear and error, e.g. velocity feedback control mode is robust to stiction, the performance of the actuator will be improved. The PI compensator in the velocity loop is used to remove steady state error.

A. Motor Model

Generally, the dynamics of a motor system is governed by

$$T_m - \frac{1}{n}T_l = nJ_m \frac{d^2\theta_g}{dt^2} + nB_m \frac{d\theta_g}{dt} \tag{1}$$

$$T_m = K_i I_a - \frac{1}{n}T_l \tag{2}$$

$$Ri_a = V - K_b \frac{d\theta_m}{dt} \tag{3}$$

where θ_m , θ_g and θ_l denote the motor angle, gearbox angle and load angle, respectively. J_m is the motor rotor moment of inertia. B_m is the viscous damping ratio. T_m is the motor torque. T_l is the load torque. K_s is the compliant element spring constant. n is the gearbox ratio. K_i is the torque constant.. I_a is armature current. K_b is the back EMF constant.

In the Laplace domain, these equations may be combined and written as

$$RI_a(s) = V(s) - K_b\omega_m(s) \tag{4}$$

$$(J_m s + B_m)\omega_m(s) = K_i I_a(s) - T_l(s)/n \tag{5}$$

B. Compliant Element Model

For SEA system with gearbox reduction, the deflection θ_s of compliant element can be written as a function of the gearbox output angle θ_g and load rotation angle θ_l

$$\theta_s = \theta_g - \theta_l \tag{6}$$

The position of the load is determined by the output torque applied to the load T_l . The torque applied to the load T_l is due to the compliant element deflection θ_s .

$$\theta_l = T_l \frac{1}{J_l s^2} = K_s \theta_s \frac{1}{J_l s^2} \tag{7}$$

$$T_l = K_s(\theta_g - \theta_l) \tag{8}$$

The open loop transfer function from gearbox position to SEA output torque by combining the Eqs (6)~(8) can be written as:

$$\frac{T_l}{\theta_g} = \frac{K_s s^2}{s^2 + \frac{K_s}{J_l}} \tag{9}$$

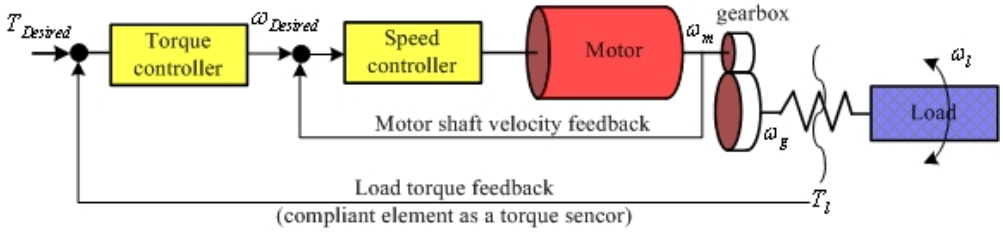

Fig. 1. The cascaded control strategy sketch map with a torque main control loop and a velocity inner loop.

C. SEA Controller Model

Two PI compensators are adopted in the cascaded control strategy. Steady state errors are removed by the two integral compensators. Different from Fig.1, the Fig.2 shows the cascaded control details with the desired velocity and voltage as follows

$$\omega_d = G_{PIo}(T_d - T_l) \tag{10}$$

$$V_d = G_{PIi}(\omega_d - \omega_m) \tag{11}$$

As a general controller, the inner and outer controllers can be written as

$$G_{PIi} = K_{PIi} + \frac{K_{ii}}{s}, G_{PIo} = K_{PIo} + \frac{K_{io}}{s} \tag{12}$$

The block diagram of the torque loop and velocity loop cascaded controlled SEA is shown in Fig.2.

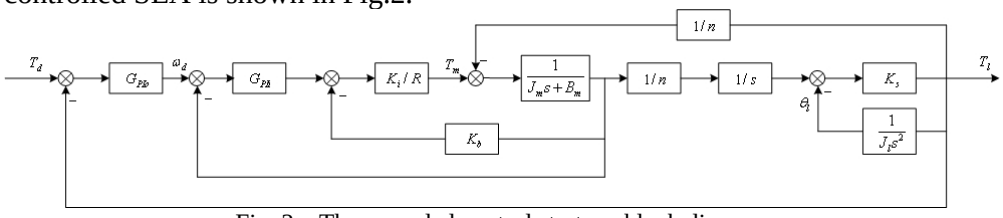

Fig. 2. The cascaded control strategy block diagram

3. Stability analysis

The most important problem in linear control systems concerns stability. Compared with a stiff actuator, besides the stability analysis of the cascaded control system, the output impedance stability of SEA should also be identified. We use two PI compensators but not two PID compensators in order to simplify the cascaded control model for getting an analytical stability boundary.

3.1 System Stability

The linear closed-loop system has closed-loop transfer function in the form:

$$\frac{T_l}{T_d} = \frac{a_{10}s^2 + a_{11}s + a_{12}}{b_{10}s^4 + b_{11}s^3 + b_{12}s^2 + b_{13}s + b_{14}} \tag{13}$$

With

$$a_{10} = \frac{K_i K_s K_{po} K_{pi}}{nR}, a_{11} = \frac{K_i K_s}{nR}(K_{po}K_{ii} + K_{pi}K_{io}), a_{12} = \frac{K_i K_s K_{ii} K_{io}}{nR}, b_{10} = J_m,$$

$$b_{11} = B_m + \frac{K_i K_b}{R} + \frac{K_i K_{pi}}{R}, b_{12} = \frac{K_S J_m}{J_l} + \frac{1}{n^2}K_s + \frac{K_i K_{ii}}{R} + K_{po}K_{pi}\frac{K_i K_s}{nR},$$

$$b_{13} = \frac{K_S B_m}{J_l} + \frac{K_i K_b K_S}{RJ_l} + \frac{K_i K_S K_{pi}}{RJ_l} + \frac{K_i K_s}{nR}(K_{po}K_{ii} + K_{pi}K_{io}),$$

$$b_{14} = \frac{K_i K_S K_{ii}}{RJ_l} + \frac{K_i K_s K_{ii} K_{io}}{nR}$$

The closed loop transfer function provides the characteristic polynomial equation. Calculating the polynomial by Routh's stability criterion, the stability of the system can be identified.

3.2 Impedance Stability

For series elastic actuator (SEA), the impedance is defined as the ratio between output torque T_l and output shaft angle θ_l. Output impedance is measure of the system stiffness for different load motion requirement. For robot motion, low impedance is recommended. Not only the impedance is a measure whether a robot system will be stable while in contact with an environment, but also the impedance is a measure of collision power. The impedance closed-loop transfer function as below

$$Z(s) = \frac{T_l}{\theta_l} = \frac{a_{20}s^4 + a_{21}s^3}{b_{20}s^4 + b_{21}s^3 + b_{22}s^2 + b_{23}s + b_{24}} \tag{14}$$

with

$$a_{20} = -K_S J_m, a_{21} = -K_S B_m, b_{20} = J_m, b_{21} = B_m + \frac{K_i K_b}{R} + \frac{K_i K_{pi}}{R},$$

$$b_{22} = \frac{K_s}{n^2} + \frac{K_i K_{ii}}{R} + \frac{K_i K_s K_{pi} K_{po}}{nR}, b_{23} = \frac{K_i K_s}{nR}(K_{po}K_{ii} + K_{pi}K_{io}), b_{24} = \frac{K_i K_s K_{ii} K_{io}}{nR}$$

Colgate[13] and Hogan[14] proved that a system will be stable when contact with unknown environment if the impedance $Z(s)$ obeys two rules:

1、Z(s) has no poles in the right half plane (Z(s) is stable);

2、The imaginary part of $Z(j\omega)$ is negative for all frequencies ω.

The first rule can be identified by the Routh's stability criterion. According to the second rule,

$$\mathrm{Im}(Z(j\omega)) = r(c_7\omega^7 + c_5\omega^5 + c_3\omega^3 + c_1\omega) \tag{15}$$

with

$$r>0\,,c_7=-(\frac{K_S J_m K_i K_b}{R}+\frac{K_S J_m K_i K_{pi}}{R}),$$

$$c_5=-\frac{K_s B_m K_s}{n^2}-\frac{K_s B_m K_i K_{ii}}{R}-\frac{K_S B_m K_i K_s K_{pi} K_{po}}{nR}+\frac{K_s J_m K_i K_s K_{po} K_{ii}}{nR}+\frac{K_s J_m K_i K_s K_{pi} K_{io}}{nR}$$

$$,c_3=\frac{K_S B_m K_i K_s K_{ii} K_{io}}{nR},c_1=0$$

The imaginary part of Z($j\omega$) can not be negative for all frequencies, especially for the low frequency because of the influence of c_3. Williamson[2] deals with this by rolling off the integral term at low frequencies leading to the analysis of control system much complicated. It is possible to symbolic analyze the system characteristic during wide frequency range without considering this.

3.3 Stable Boundary and Simulation

According to the stable rules of control system and output impedance, a possible boundary for easy tuning of the controllers is

$$\left(\frac{K_{pi}}{K_{ii}}>\frac{J_m}{B_m}\right)\wedge\left(\frac{K_{po}}{K_{io}}>\frac{J_m}{B_m}\right)\wedge$$

$$\wedge\left(K_{po}>\max(\frac{\frac{RJ_m K_{pi}}{K_{ii}}}{\frac{K_{pi}(RB_m+K_i K_b+K_i K_{pi})}{K_{ii}K_{io}}-\frac{RJ_m}{K_{io}}T_{i1}},\frac{RB_m K_{io}}{K_i K_{ii}}+\frac{K_b K_{io}}{K_{ii}})\right) \quad (16)$$

Fig.3. shows the response of the actuator to a desired torque signals in period of 1 second. The desired sinusoid torque signal is with amplitude 2Nm and frequency 50rad/s. The desired velocity signal and response are also shown in Fig.4. As shown in Fig.3 and Fig.4, the actuator can successfully follow the desired torque signal and desired velocity signal.

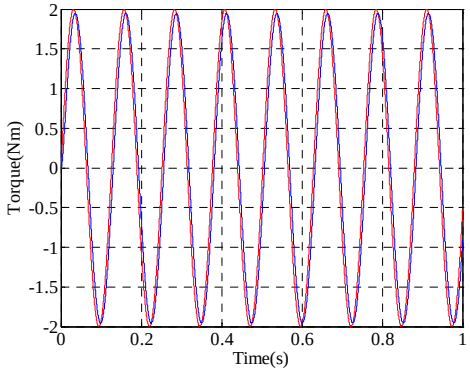

Fig. 3. Commanded and actual torque signal response

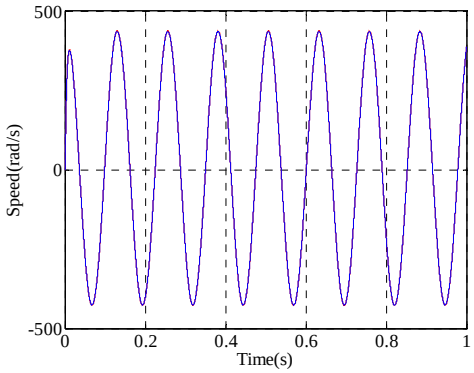

Fig. 4. Commanded and actual velocity signal response

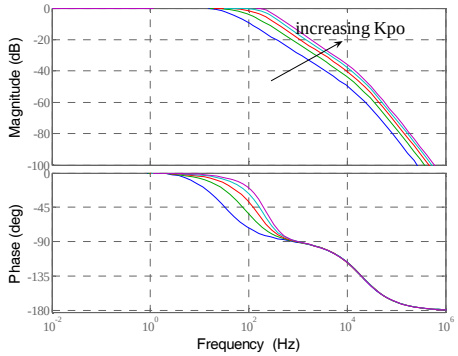

Fig. 5. The change of system bandwidth with increasing the outer-loop gain

A compliant element in the joint will decrease the bandwidth of the system, but the bandwidth is not absolutely dependant on the spring constant. As ir can be seen in Fig.5, in order to maintain a high closed-loop bandwidth, increasing the control gain can compensate the decreasing of the system bandwidth.

4. Impedance Analysis

For a robot actuator, especially for the bipedal walking robot, the ideal characteristics are with the zero output impedance and infinite bandwidth. However, it is impossible to achieve these requirements simultaneously since they conflicts with each other. Thus we need to tradeoff between the small impedance and high bandwidth. In the following, we focus on how to decrease the impedance as low as possible, meanwhile, maintaining a sufficient high bandwidth.

The following equation, which is reformulation of Eqn. (14), defines the output impedance in a dimensionless type:

$$\overline{Z}(s) = \frac{T_l}{K_s \theta_l} = \frac{a_{20}^{'} s^4 + a_{21}^{'} s^3}{b_{20} s^4 + b_{21} s^3 + b_{22} s^2 + b_{23} s + b_{24}} \tag{17}$$

where $a_{20}^{'} = -J_m$, and $a_{21}^{'} = -B_m$. The other coefficients in the equation are the same with the ones in equation (14). The Bode plot is shown in Fig. 6.

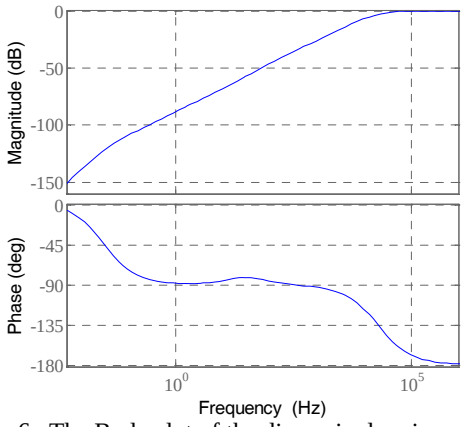

Fig. 6. The Bode plot of the dimensionless impedance.

From Fig. 6, we can see that the impedance is almost zero at low frequencies and increases as the frequency grows. At a high frequency, the impedance almost reaches the spring constant K_s of the compliant element. The analytical results are similar as the published work in Robinson's research[5].

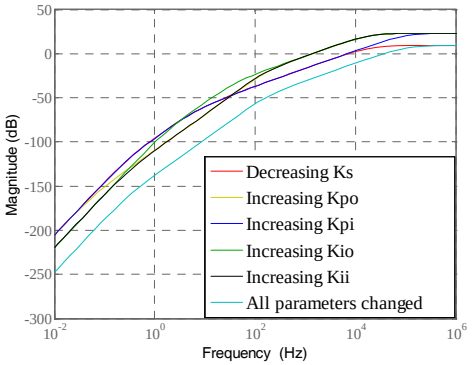

Fig. 7. The impedance magnitude plot decreasing by changing the parameters.

As it can be seen from Eqn. (17), there are five ways to decrease the output impedance for the SEA. Although the analytical results are similar, the

method in this paper has some advantages over Robinson's research, such as, there are more parameters can be tuned to decrease the impedance. In summary, the approaches to decrease the impedance are listed as follows:

(1) Decrease the compliant element spring constant

Decreasing the compliant element spring constant can significantly reduce the impedance of system, but it requires a higher control gain to maintain the system bandwidth.

(2) Increase the torque-loop control gain

As can be seen from Fig.8, changing torque-loop control gain can significantly reduce the impedance at the low and middle frequencies.

(3) Increase the velocity-loop control gain

Increasing the velocity-loop control gain can largely change the impedance at middle and high frequency. Compared with the traditional one loop control method[5], cascaded control method providing another effective method to reduce system output impedance. And also, Increase the inner loop control gain can get fast velocity-loop response.

(4) Increase the torque-loop integral gain

The research of Robinson shows that by increasing the integral gain or increasing the derivate gain can reduce the output impedance, but actually, the effect is not significant.

(5) Increase the velocity-loop integral gain.

Compared with the effect of increasing the torque-loop integral gain, increasing this parameter performs better.

5. Collision force analysis

Impact is an important phenomenon for the robot system. When a robot works in an unknown environment, it is prone to impact the surroundings. The interaction power between the robot system and the surroundings will be potentially dangerous to the robot and the environment[1]. Thus, in this paper, in order to investigate the collision characteristic, the collision force against a rigid environment between the rigid and compliant system is presented. Furthermore, for a structure-fixed compliant system, the parameters' influences are also derived. Because of the analysis complexity of collision, impulse and momentum theory are adopted.

According to theoretical mechanics, the time rate of change of the particle's angular momentum about point o is equal to the moment about point o of the force acting on the particle.

$$\frac{d}{dt}\boldsymbol{M}_o\left(m\boldsymbol{v}\right)=\boldsymbol{r}\times m\dot{\boldsymbol{v}}=\boldsymbol{M}_o\left(\boldsymbol{F}\right) \tag{18}$$

Here, $\boldsymbol{r}$ denotes the position vector drawn from point o to the particle p, and $m\boldsymbol{v}$ is the momentum of the particle p.

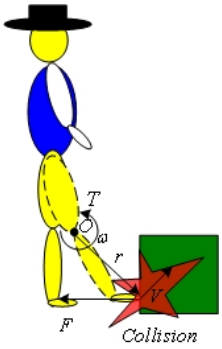

Fig. 8. Schematic diagram of collision

Consider the rigid limb, which is rotating about the mimetic joint output axis. The limb can be treated as a mass point particle p with the mass moment of inertia about the mimetic joint output axis J_o. The angular velocity is ω and the external force is F.

Neglecting the friction of the system, we differentiate the equation of angular momentum of a rotating particles system

$$\frac{d}{dt}\left(J_o\boldsymbol{\omega}\right)=\boldsymbol{M}_o\left(\boldsymbol{F}\right) \tag{19}$$

The differential ratio of momentum between rigid joint system and compliant joint system is shown in Eqn. (20). The footnotes r and c denote rigid joint and compliant joint, respectively.

$$\frac{\dfrac{d}{dt}\boldsymbol{M}_{or}\left(m\boldsymbol{v}\right)}{\dfrac{d}{dt}\boldsymbol{M}_{oc}\left(m\boldsymbol{v}\right)}=\frac{\boldsymbol{M}_{or}\left(\boldsymbol{F}\right)}{\boldsymbol{M}_{oc}\left(\boldsymbol{F}\right)}=\frac{\boldsymbol{r}\times\boldsymbol{F}_{or}}{\boldsymbol{r}\times\boldsymbol{F}_{oc}}=\frac{\dfrac{d}{dt}\left(J_{or}\boldsymbol{\omega}\right)}{\dfrac{d}{dt}\left(J_{oc}\boldsymbol{\omega}\right)} \tag{20}$$

In order to analyze the collision force between the rigid system and the compliant system, the equations can be written as scalar quantity form by assuming that the situations of the collision are the same. According to the definition of impedance, the equivalent mass moment of inertia in Laplace domain can be written as

$$J_l^{'}=\frac{T_l}{\theta_l s^2}=\frac{Z(s)\cdot\theta_l}{\theta_l s^2}=\frac{Z(s)}{s^2} \tag{21}$$

By combing these equations, we have the following one:

$$\frac{M_{oc}\left(mv\right)\left(s\right)s}{M_{or}\left(mv\right)\left(s\right)s}=\frac{J_{oc}\theta_{lc}\left(s\right)s^2}{J_{or}\theta_{lr}\left(s\right)s^2}=\frac{Z_{oc}\left(s\right)}{Z_{or}\left(s\right)} \tag{22}$$

That means the collision force can be judged by the impedance

$$\frac{Z_{oc}(s)}{Z_{or}(s)} = \frac{a_{30}s^2 + a_{31}s + a_{32}}{b_{30}s^4 + b_{31}s^3 + b_{32}s^2 + b_{33}s + b_{34}} \tag{23}$$

with

$$a_{30} = \frac{1}{n^2} + \frac{K_i K_{p1} K_{p2}}{nR}, a_{31} = \frac{K_i}{nR}\left(\frac{K_{p1}}{T_{i2}} + \frac{K_{p2}}{T_{i1}}\right), a_{32} = \frac{K_i}{nRT_{i1}T_{i2}}, b_{30} = J_m / K_s,$$

$$b_{31} = B_m / K_s + \frac{K_i K_b}{RK_s} + \frac{K_i K_{p2}}{RK_s}, b_{32} = \frac{1}{n^2} + \frac{K_i}{RT_{i2}K_s} + \frac{K_i K_{p1} K_{p2}}{nR},$$

$$b_{33} = \frac{K_i}{nR}\left(\frac{K_{p1}}{T_{i2}} + \frac{K_{p2}}{T_{i1}}\right), b_{34} = \frac{K_i}{nRT_{i1}T_{i2}}$$

Fig.9. shows that, at a low frequency, the collision force difference between rigid system and compliant system is not significant. That is the reason why the rigid robot systems slow down the work speeds before collision by programming beforehand. But, as the frequency increases, the compliant joint performs better and better. Moreover, decreasing the spring constant of the compliant element can refine the performance of the compliant joint.

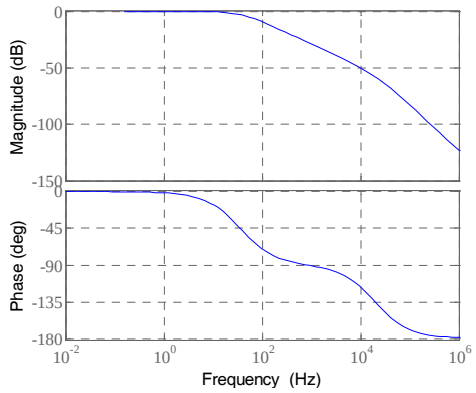

Fig. 9. Bode plot of collision force ratio between rigid system and compliant

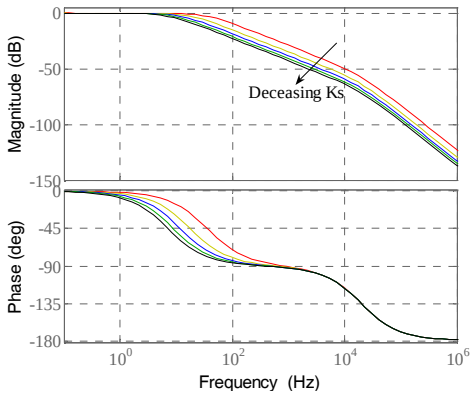

Fig. 10. The Bode plot changing by decreasing the compliant element spring constant

For a compliant element fixed system, the spring constant can no longer be changed. The emphasis on minimize the collision force is on the parameters changing. For the cascaded control SEA above, according to the Eqn. (23), the ratio between the impedance to be changed and the initial system impedance can be written as

$$\frac{\bar{F}_{oc}}{F_{oc}}=\frac{\bar{Z}_c}{Z_c} \tag{24}$$

Fig.11. shows the Bode plot change trend by increasing the controller gains. In order to reduce the impact power, we can fulfill this by reducing the output impedance. Low impedance means low system stiffness, the collision time will be prolonged.

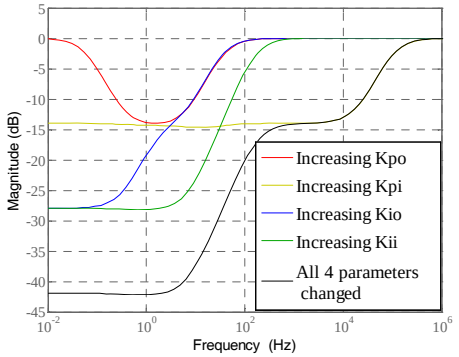

Fig. 11. Magnitude plot changing by increasing the controller gains

6. Saturation Influence

Because of the limitation of the DC velocity and commanded voltage, these is a sudden change of signals that over the recommended amplitude are not desired. Actuator saturation has to be avoided to keep the performance of the system. Saturation operators are designed to set the limitation for commanded DC velocity and voltage.

In the two controllers, there are two integral saturation operators, one velocity saturation operator, one voltage saturation operator in sum. The schematic diagram of saturation operator is shown in Fig.12[12], in which, the input of the saturation operator, u_i, is in the range $u_{lmin} \le u_i \le u_{lmax}$. The saturation operator output, u_o, is limited as $u_l \le u_o \le u_h$. The parameters u_{lmin}, u_{lmax}, u_l and u_h in Fig. 12. are constant. Every point in the saturation band equals to an equivalent gain in the linear system model.

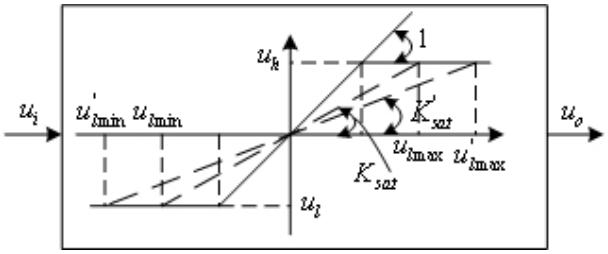

Fig. 12. Schematic diagram of a saturation operator.

The schematic diagrams of the nonlinear torque controller and nonlinear velocity controller are shown in Fig.13. and Fig.14, respectively. The range limitations of equivalent gains of the integral saturation operator in torque loop, velocity saturation operator, integral saturation operator in velocity loop and voltage saturation operator are in Eqns. (25)(26)(27)(28), respectively.

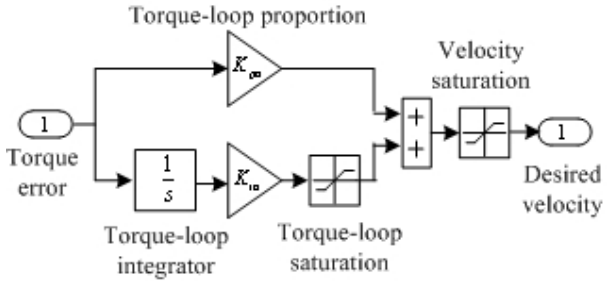

Fig. 13. Schematic diagram of the nonlinear torque controller with saturation operator

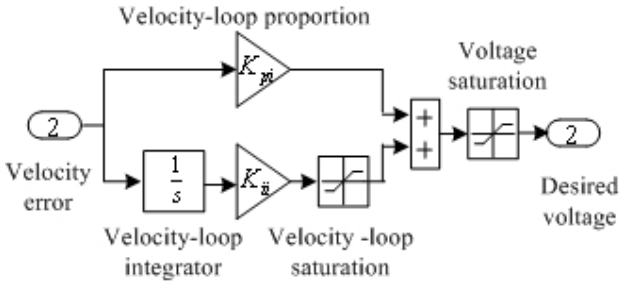

Fig. 14. Schematic diagram of the nonlinear velocity controller with saturation operator

$$0 \le \frac{u_{hinto}}{K_{po}(T_{dmax} - T_{dmin})} \le K_{satinto} \le 1 \tag{25}$$

$$0 \le \frac{u_{hvel}}{K_{po}(T_{dmax} - T_{dmin}) + u_{hinto}} \le K_{satvel} \le 1 \tag{26}$$

$$0 \le \frac{u_{hinti}}{K_{pi}(u_{hvel} - u_{lvel})} \le K_{satinti} \le 1 \tag{27}$$

$$0 \le \frac{u_{hvol}}{K_{pi}(u_{hvel} - u_{lvel}) + u_{hinti}} \le K_{satvol} \le 1 \tag{28}$$

For a nonlinear torque controller, assuming $K_{p1}^{'} > K_{p1}$, the corresponding equivalent gain

$$\left[\frac{u_{hvel}}{K_{p1}(T_{dmax} - T_{dmin}) + u_{hint1}}, 1\right] \subset \left[\frac{u_{hvel}}{K_{p1}^{'}(T_{dmax} - T_{dmin}) + u_{hint1}}, 1\right] \tag{29}$$

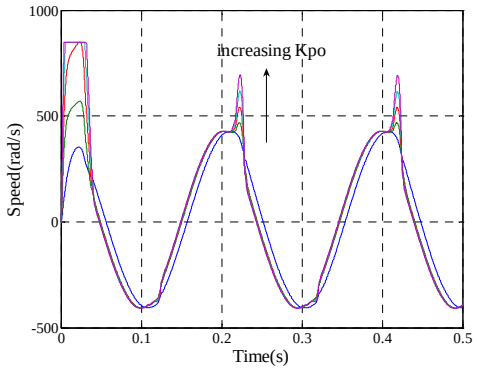

Fig. 15. The response trend of torque signal by increasing the controller gain

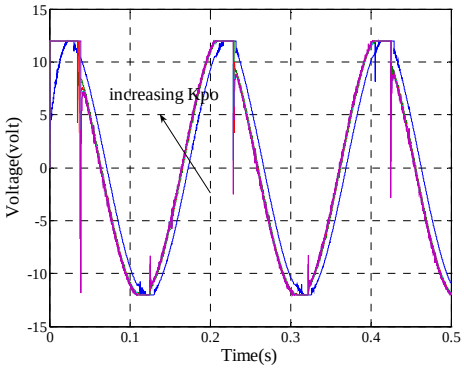

Fig. 16. the response trend of velocity signal by increasing the controller gain

This means that increasing the proportional gain will expanded the equivalent gain range. For given signals, increased proportional gain could speed up the response, but easy to get saturation performance, resulting in an inaccurate control, this result is not expected.

7. Conclusions

In this paper, a cascade controller for a compliant actuator has been designed. There are two sub-controllers in the cascade control strategy who provide four parameters to regulate the characteristic. By analyzing the stability of the control system model and output impedance, simple boundaries for the control system parameters are derived.

For a compliant joint, a large force bandwidth requires a high spring constant which would lead to a high impedance. When the robot system contacts with an unknown surroundings, in order to reduce the impact force, a low output impedance of the compliant system is required. From the analytical results in this paper, we can conclude that, for one structure-fixed model, in order to decrease the impedance and collision force, the controller parameters should be changed in principle. But these changes may induce the actuator saturation. Therefore, the design of the controller parameters should tradeoff between these conflicting requirements.

R E F E R E N C E S

[1]. *D.W. Robinson,* Design and Analysis of Series Elasticity in Closed-loop Actuator Force Control, PhD Thesis, Department of Mechanical Engineering, Massachusetts Institute of Technology, 2000.

[2]. *M.M. Williamson,* Series Elastic Actuators, Master of Science Thesis, Department of Electrical Engineering and Computer Science, Massachusetts Institute of Technology, 1995.

[3]. *G.A. Pratt, M.M. Williamson,* Series Elastic Actuators, IEEE International Conference on Intelligent Robots and Systems, **vol.1**,1995, pp.399-406.
[4]. *G.A. Pratt, M.M. Williamson, P. Dillworth, J. Pratt, K. Ulland, and A. Wright,* Stiffness Isn't Everything, In Fourth International Symposium on Experimental Robotics, ISER 95, 1995.
[5]. *D.W. Robinson, J.E. Pratt, D.J. Paluska, and G.A,* Pratt. Series Elastic Actuator Development For A Biomimetic Walking Robot, In 1999 IEEE/ASME International Conference on Advanced Intelligent Mechatronics, 1999, pp.561-568.
[6]. *G.A. Pratt, P. Williamson, C. Bolton, and A. Hofman,* Late Motor Processing in Low-Impedance Robots: Impedance Control of Series Elastic Actuators, presented at Proceedings of American Control Conference, **Vol.4**, 2004, pp.3245-3251.
[7]. *R. Van Ham, B. Vanderborght, M. Van Damme, B. Verrelst, and D. Lefeber,* Maccepa: the Mechanically Adjustable Compliance and Controllable Equilibrium Position Actuator: Design and Implementation in a Biped Robot, Robotics and Autonomous Systems, **Vol.55**, no.10, 2007, pp.761-768.
[8]. *H. Herr, A. Wilkenfeld, and J. Blaya,* Patient-adaptive Prosthetic and Orthotic Leg Systems, In Proceedings of the 12th Nordic Baltic Conference on Biomedical Engineering and Medical Physics, June, 2002, pp. 123–128.
[9]. *M. Kim, J. Weber, and S. Cha,* A Design of a Modular Force Sensing Robot Arm for Self-Assembling Robots in a System, In Proceedings of Robotics and Applications, August 2006, pp.132-137.
[10]. *H. Vallery, R. Ekkelenkamp, H. van der Kooij and M. Buss,* Passive and Accurate Torque Control of Series Elastic Actuators, IEEE/RSJ International Conference on Intelligent Robots and Systems, 2007, pp.3534 – 3538.
[11]. *G. Wyeth,* Demonstrating the Safety and Performance of a Velocity Sourced Series Actuator, IEEE International Conference on Robotics and Automation, 2006, pp.3642-3647.
[12]. *R. Ghorbani,* On Controllable Stiffness Bipedal Walking, PhD Thesis, Department of Mechanical and Manufacturing Engineering, The University of Manitoba, 2008.
[13]. *E. Colgate, N. Hogan,* An analysis of Contact Instability in Terms of Passive Equivalents, IEEE International Conference on Robotics and Automation, 1989, pp.404-409.
[14]. *N. Hogan,* On the Stability of Manipulators Performing Contact Tasks, IEEE Journal of Robotics and Automation, **Vol. 4**, No. 6, December 1988, pp.677-686.